

Matrix Cooling for Gas Turbine Blades

Jinu Chandran¹, Nikhil Chitnavis², Himani Garg³

¹Research Scholar, Department of Mechanical Engineering, BITS Pilani, K.K. Birla Goa Campus, India

²Research Assistant, FOSSEE Project, IIT Bombay, India

³Assistant Professor, Department of Energy Sciences / Heat Transfer, Lund University, Sweden

Abstract

The present study conducts a computational investigation of turbulent flow and heat transfer characteristics within a latticework cooling structure operating under a turning flow configuration, using OpenFOAM v2312 with the SST $k-\omega$ turbulence model. The turning flow configuration is particularly relevant to trailing-edge cooling applications in gas turbine blades, where coolant flow undergoes a significant directional change before entering the latticework region. The computational domain comprises a smooth inlet channel followed by a latticework section with inclined ribs, generating multiple subchannels and complex flow turning with vortex interactions. Simulations are performed for mass flow rates ranging from 0.0139 kg/s to 0.0669 kg/s to evaluate total Nusselt number distributions, pressure losses, and velocity fields. The analysis examines the effects of flow turning on heat transfer enhancement, flow distribution between upper and lower subchannels, and the associated pressure losses. The results provide detailed insights into the relationship between nonuniform flow distribution, vortex dynamics, and thermal performance, supporting the optimisation of trailing-edge cooling designs in gas turbine blades.

1. Introduction

The continuous demand for higher thermal efficiency in modern gas turbines has led to significant increases in turbine inlet temperatures, often exceeding the material limits of critical components such as high-pressure turbine blades. Advanced internal cooling techniques ensure reliable operation under such extreme conditions. Among various internal cooling strategies, latticework cooling structures have emerged as a promising solution due to their superior heat transfer performance and structural rigidity. These structures consist of intersecting ribs that form a network of subchannels,

significantly increasing the wetted surface area and promoting complex vortex interactions that enhance convective heat transfer.

Latticework cooling channels can be implemented in turbine blades leading and trailing edge regions, where efficient heat dissipation is crucial. However, the effectiveness of these structures is highly dependent on the flow configuration, which governs how coolant enters and interacts within the latticework region. While the previous studies have primarily focused on radial flow configurations Bunker, 2004, Hagari and Ishida, 2013 and cross flow configurations, the turning flow configuration (TFC), which is particularly relevant to trailing edge cooling applications, remains relatively less explored.

In TFC, the coolant undergoes a directional change before entering the latticework structure, introducing complex flow phenomena such as large-angle flow turns, nonuniform flow distribution, and strong vortex interactions between adjacent subchannels. These characteristics significantly influence local heat transfer distributions and pressure loss behaviour, making it a critical area of investigation for optimising turbine blade cooling systems.

2. Problem Statement

The present study aims to computationally investigate the turbulent flow and heat transfer behaviour within a latticework cooling structure operating under TFC, using OpenFOAM version 2312. This configuration is particularly relevant to turbine blade trailing-edge cooling, where the coolant undergoes a directional change before entering the latticework region.

The computational domain includes a smooth inlet channel connected to a latticework section composed of inclined ribs that form intersecting subchannels. The geometric configuration and operating parameters—such as rib inclination, subchannel hydraulic diameter, and range of mass flow rates from 0.0139 kg/s to 0.0669 kg/s—are based on a previously published study to ensure physical relevance and practical applicability Luo et al., 2021.

The primary objective is to analyse the resulting flow field characteristics, Nusselt number distributions, and pressure losses associated with the TFC. The simulations employ the Shear Stress Transport (SST) $k-\omega$ turbulence model to resolve the complex flow features arising from abrupt directional changes and rib-induced turbulence. This model enables accurate resolution of near-wall behaviour and vortex structures, which are critical to heat transfer enhancement in such geometries.

The study focuses on quantifying how variations in mass flow rate influence heat transfer distribution, examining the role of flow turning and nonuniform flow distribution on pressure drop and thermal enhancement. The work aims to provide detailed insights into the flow dynamics and

their impact on heat transfer distribution in the TFC latticework configuration through detailed analysis of velocity fields, streamlines, and surface heat transfer distributions.

3. Governing Equations

The numerical simulations in this study solve the steady-state, incompressible Reynolds-Averaged Navier–Stokes (RANS) equations using the Boussinesq approximation to account for buoyancy effects. The governing equations for mass, momentum, and energy conservation are expressed as follows.

Continuity equation:

$$\nabla \cdot \mathbf{U} = 0 \quad (1)$$

Momentum conservation:

$$\rho(\mathbf{U} \cdot \nabla)\mathbf{U} = -\nabla p + \nabla \cdot \left[\mu_{\text{eff}} \left(\nabla \mathbf{U} + (\nabla \mathbf{U})^T \right) \right] + \mathbf{f}_b \quad (2)$$

where the body force due to buoyancy is defined under the Boussinesq approximation as:

$$\mathbf{f}_b = -\rho\beta\mathbf{g}(T - T_{\text{ref}}) \quad (3)$$

Energy conservation:

$$\rho c_p (\mathbf{U} \cdot \nabla T) = \nabla \cdot (k_{\text{eff}} \nabla T) \quad (4)$$

where \mathbf{U} is the velocity vector, p is pressure, ρ is the fluid density (constant except in the buoyancy term), c_p is the specific heat at constant pressure, T is temperature, μ_{eff} and k_{eff} are the effective dynamic viscosity and thermal conductivity, β is the thermal expansion coefficient, and \mathbf{g} is the gravitational acceleration vector.

The Shear Stress Transport (SST) k – ω turbulence model is employed to close the RANS equations. This hybrid model combines the near-wall accuracy of the k – ω formulation with the robustness of the k – ε model in the free stream, making it suitable for flows with separation and adverse pressure gradients OpenCFD Ltd., 2024.

The transport equation for the turbulent kinetic energy k is:

$$\frac{\partial}{\partial t}(\rho k) + \nabla \cdot (\rho \mathbf{U} k) = \nabla \cdot (\rho D_k \nabla k) + \rho G - \frac{2}{3} \rho k (\nabla \cdot \mathbf{U}) - \rho \beta^* \omega k + S_k \quad (5)$$

The equation for the specific dissipation rate ω is:

$$\frac{\partial}{\partial t}(\rho\omega) + \nabla \cdot (\rho \mathbf{U}\omega) = \nabla \cdot (\rho D_\omega \nabla \omega) + \gamma G_\nu - \frac{2}{3}\gamma\omega(\nabla \cdot \mathbf{U}) - \rho\beta\omega^2 - \rho(F_1 - 1)C_{Dk\omega} + S_\omega \quad (6)$$

The turbulent eddy viscosity is calculated using:

$$\nu_t = \frac{a_1 k}{\max(a_1 \omega, b_1 F_2 S)} \quad (7)$$

Model constants and blending functions follow the OpenFOAM v2312 implementation based on the 2003 formulation by Menter et al. OpenCFD Ltd., 2024.

4. Simulation Procedure

4.1 Geometry and Mesh

The TFC latticework geometry investigated in this study, illustrated in Figure 1, represents a trailing-edge internal cooling design for turbine blades. The computational domain consists of two primary regions: a 40.0 mm-wide smooth inlet channel and a latticework section featuring ribbed subchannels arranged in a diagonal cross pattern.

The inlet channel introduces the coolant flow and redirects it into the lattice structure, thereby inducing a large-angle directional change. This transition produces two distinct inflow angles into the subchannels: subchannels on the downward side experience an effective inlet angle of 145° . In contrast, those on the upward side are approached at a shallower angle of 35° .

The latticework section is constructed using ribs inclined at an angle $\beta = 35^\circ$ for the primary flow direction. Each rib has a width $t = 4$ mm and height $H = 10$ mm, while the subchannel width $w = 10$ mm results in a square cross section with an aspect ratio of 1. The corresponding hydraulic diameter is $D_{\text{sub}} = 10$ mm, and the entire lattice extends $L = 268.5$ mm in the streamwise direction and $W_1 = 85.5$ mm in width.

Due to the limited upstream development length, some subchannels near the sidewalls do not experience complete turning and instead act as relatively straight flow passages. This inherent asymmetry in subchannel activation contributes to strong nonuniform flow distribution along the y -axis. It enhances the complexity of the internal flow field, making this configuration particularly well-suited for studying secondary flow interactions, vortex development, and heat transfer distribution.

The computational mesh was generated using `snappyHexMesh` in OpenFOAM v2312, with the base mesh initialised through `blockMesh`. The geometry was imported as an STL surface,

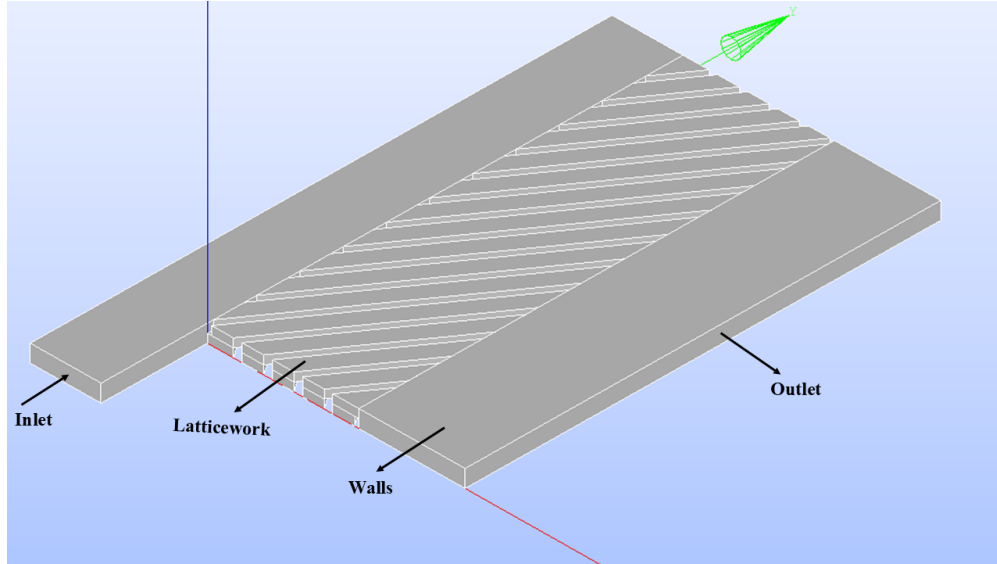


Figure 1: Geometry of Turning Flow Configuration

and castellated, snapped, and layer addition steps were used to refine the mesh near the walls and rib surfaces. Local refinement was applied within the latticework region to resolve the inclined rib-induced flow structures.

The final mesh consists of approximately 2.15 million cells, predominantly hexahedral ($\sim 91\%$), and several prisms and polyhedra used to capture complex intersections as illustrated in Figure 2. Despite the coarse resolution, wall and rib surfaces were adequately resolved to allow qualitative assessment of TFC. Mesh quality metrics obtained from `checkMesh` indicated a maximum non-orthogonality of 68.5° , and a maximum skewness of 4.13. Only one face exceeded the recommended skewness threshold. It was reported to the `skewFaces` set, suggesting that the overall mesh quality remains within acceptable limits for steady-state simulations using the `buoyantBoussinesqSimpleFoam` solver. A formal grid independence study was not performed in this work; however, the potential limitations associated with the mesh resolution are acknowledged and considered in interpreting results.

4.2 Initial and Boundary Conditions

The simulations were conducted using OpenFOAM v2312, solving the steady-state RANS equations with the SST $k-\omega$ turbulence model. The domain includes only the fluid region of the TFC latticework geometry. Air was modelled as an ideal gas with temperature-dependent density (via the Boussinesq approximation), enabling buoyancy-driven effects.

Based on an inlet channel hydraulic diameter, a range of mass flow rates from 0.0139 to 0.0669 kg/s was imposed at the inlet.

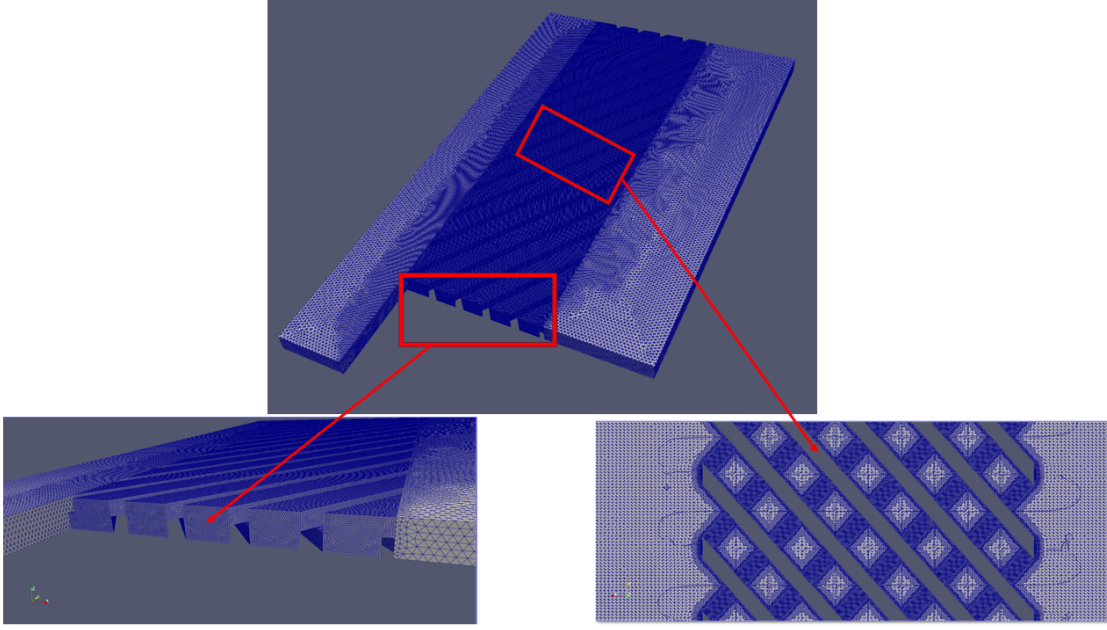


Figure 2: Overview of the structured mesh generated using `snappyHexMesh`, including zoomed views showing rib-resolved refinement near the turning junctions and subchannels.

- **Inlet:** Uniform velocity (based on flow rate), fixed temperature of 293 K, 5% turbulence intensity.
- **Outlet:** Fixed pressure (0 Pa gauge), zero gradient for all other quantities.
- **Walls (fins + primary surfaces):** No-slip condition, with selected rib walls fixed at 323 K to simulate heated surfaces; other walls treated as adiabatic.
- **Turbulence quantities:** Specified at inlet using fixed values for k , ω , ν_t , and α_t ; wall functions were applied at solid boundaries to resolve near-wall gradients.

Tables 1 and 2 summarise the boundary conditions applied to key fields. All fields were initialised using uniform values representative of ambient air conditions to support solver stability and convergence.

Table 1: Boundary conditions for velocity, pressure, and temperature

Section	U	p	p_rgh	T
Inlet	fixedValue: (28.84 0 0)	zeroGradient	zeroGradient	fixedValue: 293
Outlet	zeroGradient	fixedValue: 0	fixedValue: 0	zeroGradient
Wall_rest	noSlip	zeroGradient	zeroGradient	zeroGradient
Wall_ribs1	noSlip	zeroGradient	zeroGradient	fixedValue: 323
Wall_ribs2	noSlip	zeroGradient	zeroGradient	zeroGradient

Table 2: Boundary conditions for turbulence quantities and thermal diffusivity

Section	k	omega	nut	alphat
Inlet	fixedValue: 3.119	fixedValue: 1577	fixedValue: 0.00198	fixedValue: 0
Outlet	zeroGradient	zeroGradient	zeroGradient	zeroGradient
Wall_rest	kqRWallFunction: 3.119	omegaWallFunction: 1577	nutkWallFunction: 0.00198	alphatJayatilleke WallFunction: 0
Wall_ribs1	kqRWallFunction: 3.119	omegaWallFunction: 1577	nutkWallFunction: 0.00198	alphatJayatilleke WallFunction: 0
Wall_ribs2	kqRWallFunction: 3.119	omegaWallFunction: 1577	nutkWallFunction: 0.00198	alphatJayatilleke WallFunction: 0

4.3 Solver

The simulations were performed using the steady-state buoyant solver *buoyantBoussinesqSimpleFoam*, which is designed for low Mach number incompressible flows with buoyancy effects under the Boussinesq approximation. The solver configuration ensured second-order accuracy in spatial discretisation while maintaining numerical stability. Gradient terms were handled using the Gauss linear scheme, and divergence terms were treated with a bounded Gauss upwind scheme for convection and Gauss linear for diffusion. Laplacian terms were discretised using the Gauss linear corrected scheme to account for non-orthogonality in the mesh, and linear interpolation was employed for face-centred values. The temporal treatment was steady-state, using the steadyState time scheme.

For equation solvers and controls, pressure–velocity coupling was managed using the SIMPLE algorithm. Pressure was solved using the Preconditioned BiCGStab (PBiCG) method with a DILU preconditioner. In contrast, velocity and turbulence equations were solved using the smoothSolver and PBiCG methods with appropriate convergence tolerances. Under-relaxation factors of 0.3, 0.7, and 0.5 were applied to pressure, velocity, temperature and turbulence, respectively. The simulation was advanced until all residuals dropped below 10^{-5} or until a maximum of 1000 iterations was reached.

5. Results and Discussions

The simulation results provide a detailed picture of the flow field and thermal behaviour within the latticework cooling structure under TFC. Velocity contour plots (Figure 3) reveal a strong asymmetry between the top and bottom subchannels, caused by the directional change in flow at the inlet. Downward-facing subchannels exhibit significantly higher velocities due to more favourable flow alignment (145° entry), while top subchannels receive comparatively lower momentum. This nonuniform distribution leads to imbalanced heat transfer across the lattice.

Streamline visualisations (Figure 4) further demonstrate the complex secondary flow structures of the subchannels and the strong vortex interactions. Recirculation zones and crossflow between adjacent channels are observed, particularly at rib junctions, contributing to enhanced mixing and localised heat transfer. The SST $k-\omega$ turbulence model captures these vortical features and the associated flow separation along the rib surfaces.

The pressure loss across the latticework region increases with the mass flow rate, as shown in Figure 5. The pressure drop displays a non-linear trend for Reynolds number, reflecting increased viscous losses and flow separation effects at higher velocities. Despite using a coarse mesh, the trend and magnitudes are consistent with physical expectations for ribbed channel flows under turning configurations.

The total Nusselt number (Figure 6) also increases with the mass flow rate, reflecting improved convective heat transfer due to stronger turbulence and vortex generation. However, the enhancement is not uniform across all subchannels, highlighting the influence of nonuniform flow distribution. Localised underperformance in some regions may be attributed to inadequate flow penetration, especially in the upper subchannels, where the flow turning is more abrupt and less aligned with the rib orientation.

Although the simulation captures key flow and heat transfer trends, using a coarse mesh (~ 2 million cells) introduces some limitations in fully resolving near-wall gradients and fine-scale turbulence structures, which eventually contributes to conservative predictions of the Nusselt number, particularly at higher Reynolds numbers. However, the results are qualitatively consistent with the expected behaviour and support the effectiveness of the TFC latticework design in promoting heat transfer through vortex-induced mixing.

The numerical study demonstrates the impact of the inlet flow turning on the internal flow distribution, pressure loss, and thermal performance in latticework cooling structures. The findings offer insight into the flow physics that governs trailing-edge cooling applications and highlight areas for future refinement, including mesh resolution and local heat transfer contour evaluation.

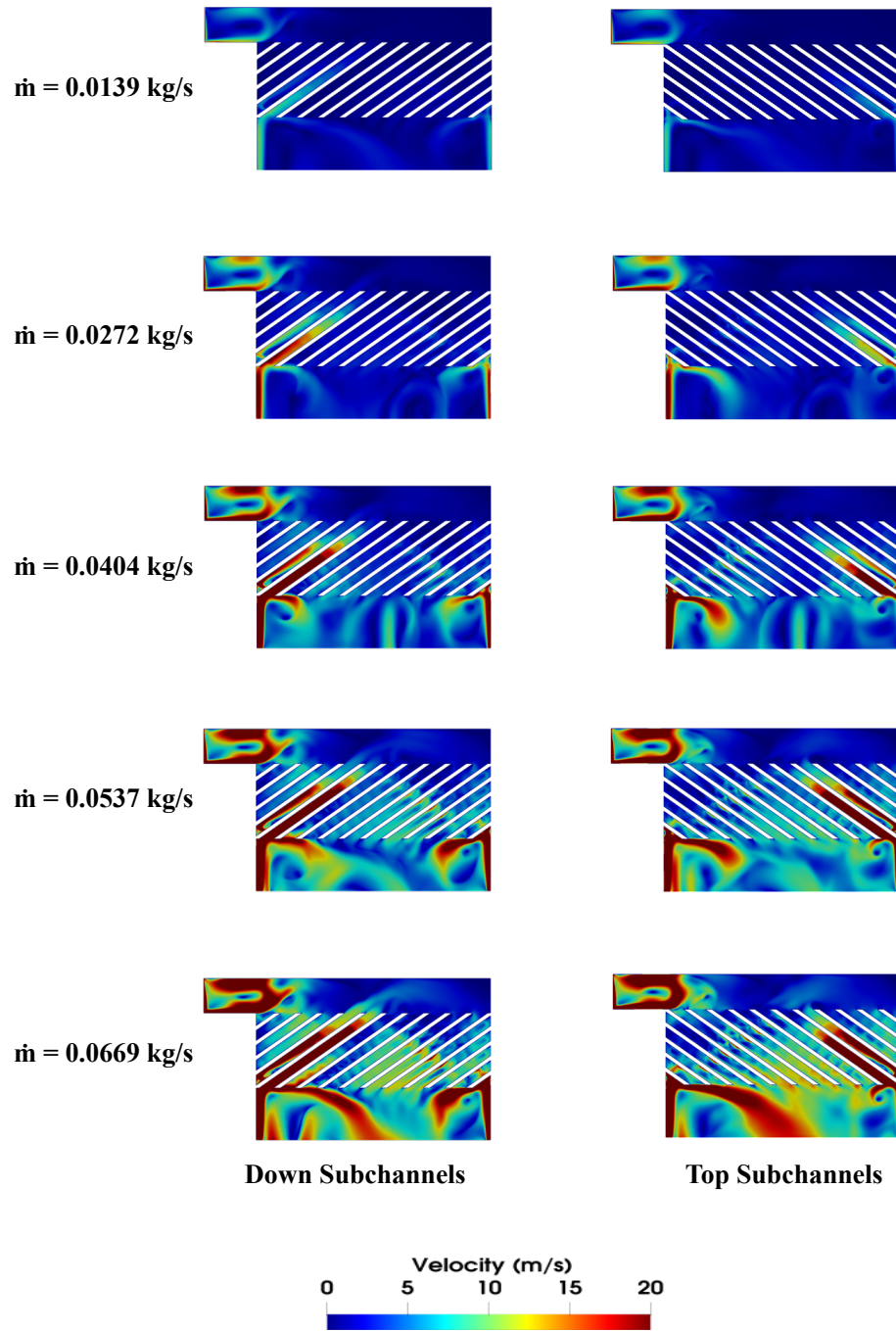


Figure 3: Velocity contours at selected planes showing flow distribution across top and down subchannels

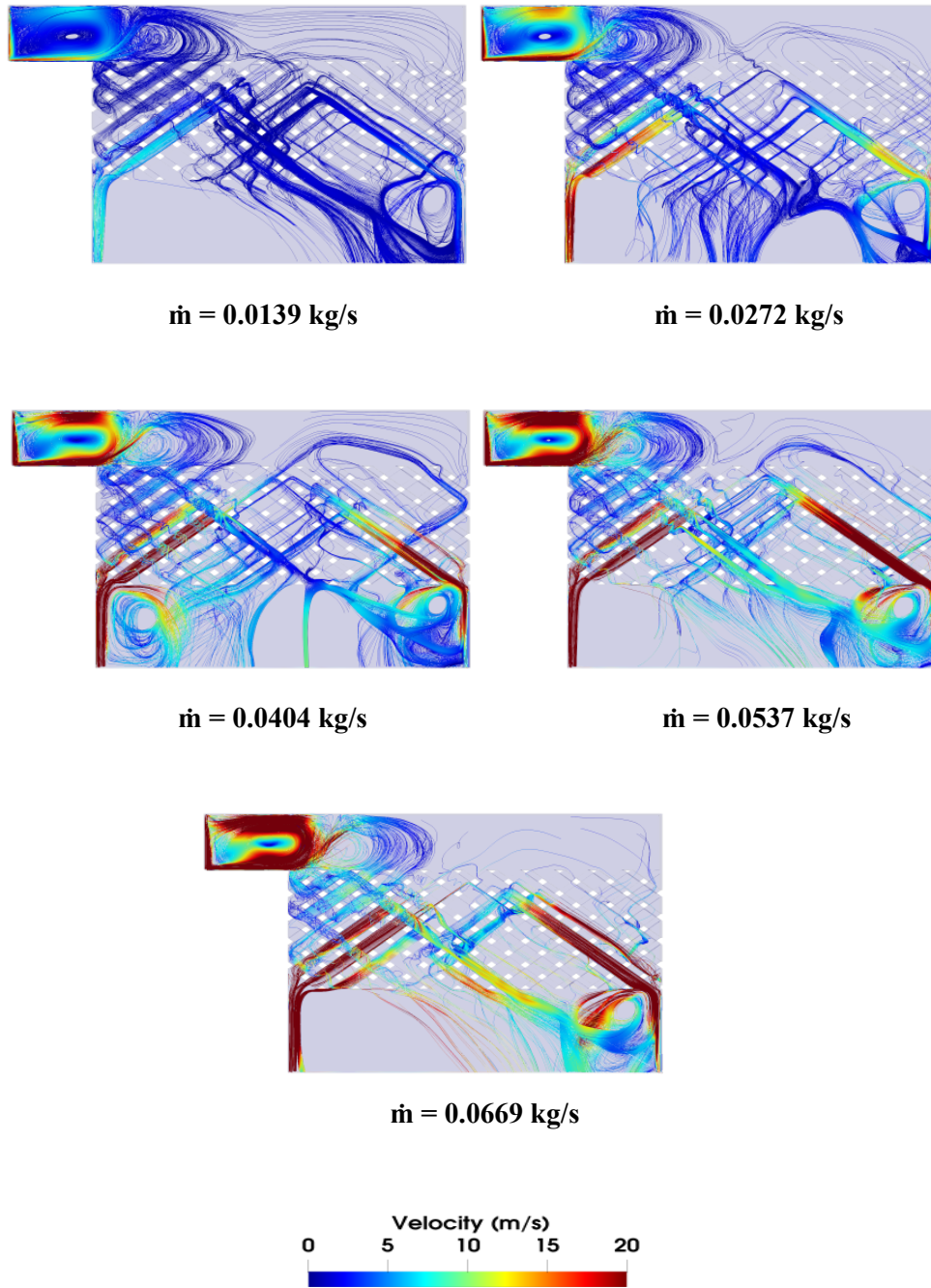


Figure 4: Streamline visualisation highlighting secondary flow structures and vortex interactions within the latticework

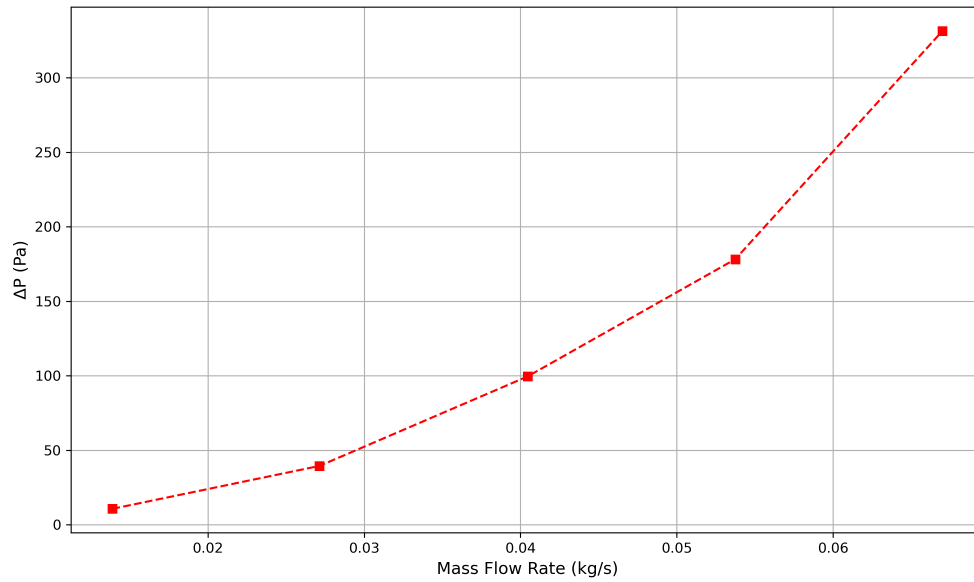


Figure 5: Pressure loss across the latticework cooling structure for varying mass flow rates

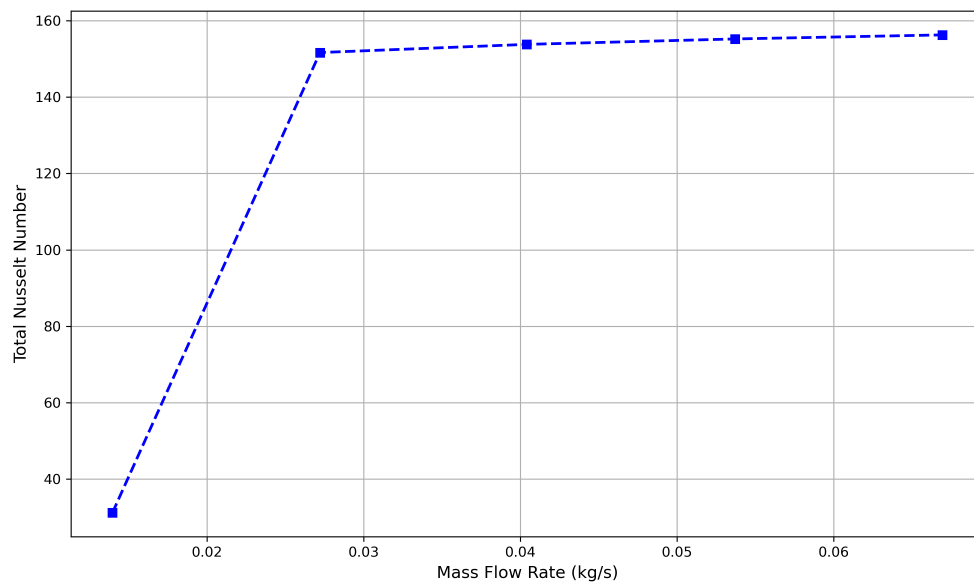


Figure 6: Variation of total Nusselt number with mass flow rate in the TFC latticework configuration

6. Conclusion and Future Work

This study used OpenFOAM to conduct a computational investigation of turbulent flow and heat transfer in a latticework cooling structure under TFC, representing trailing-edge turbine blade cooling. The simulations were performed at various mass flow rates, successfully capturing key

physical phenomena, including nonuniform flow distribution, secondary vortex generation, and pressure loss characteristics unique to the TFC geometry.

The SST $k-\omega$ model effectively resolved large-scale flow structures and heat transfer trends. The velocity and streamline plots highlighted the asymmetrical channel behaviour, while the Nusselt number and pressure drop trends followed expected physical behaviour with increasing Reynolds number. Despite mesh limitations, the results qualitatively reflect the performance of TFC geometries and provide valuable insights into the role of flow turning in thermal enhancement.

For future work, improvements could include mesh refinement to enable quantitative validation and incorporation of local Nusselt number contour mapping for surface-level heat transfer analysis.

Acknowledgement

I am sincerely grateful to the FOSSEE team for giving me the unique opportunity to participate in the Summer Fellowship program. I want to express my heartfelt thanks to my guide, **Prof. Himani Garg**, for her constant support, guidance, and encouragement throughout the project. Her expertise in Computational Fluid Dynamics and heat transfer has significantly improved my understanding of this intricate field and inspired me to continue exploring it with greater curiosity.

I am also grateful to my mentor, **Mr. Nikhil Chitnavis**, for his valuable mentorship, practical advice, and insightful suggestions on OpenFOAM and simulation workflow.

References

- Bunker, R. S. (2004, June). *Latticework (vortex) cooling effectiveness: Part 1 — stationary channel experiments* (Vol. Volume 3: Turbo Expo 2004). <https://doi.org/10.1115/GT2004-54157>
- Hagari, T., & Ishida, K. (2013, June). *Numerical investigation on flow and heat transfer in a lattice (matrix) cooling channel* (Vol. Volume 3A: Heat Transfer). <https://doi.org/10.1115/GT2013-95412>
- Luo, J., Rao, Y., Yang, L., Yang, M., & Su, H. (2021). Computational analysis of turbulent flow and heat transfer in latticework cooling structures under various flow configurations. *International Journal of Thermal Sciences*, 164, 106912.
- OpenCFD Ltd. (2024). Openfoam user guide: K-omega shear stress transport (sst) model. <https://www.openfoam.com/documentation/user-guide>